

Photocatalytic degradation of methylene blue using Zn/SBA-15 synthesized from palm oil fuel ash

Nur Fatimah Mohamad Zahir¹, Herma Dina Setiabudi^{1*}, Rohayu Jusoh¹, Nur Hidayatul Nazirah Kamarudin²

¹Faculty of Chemical and Process Engineering Technology, Universiti Malaysia Pahang, Lebuhraya Tun Razak, 26300 Gambang, Kuantan, Pahang, Malaysia

²Department of Chemical and Process Engineering, Faculty of Engineering & Built Environment, Universiti Kebangsaan Malaysia, 43600 Bangi, Selangor Darul Ehsan, Malaysia.

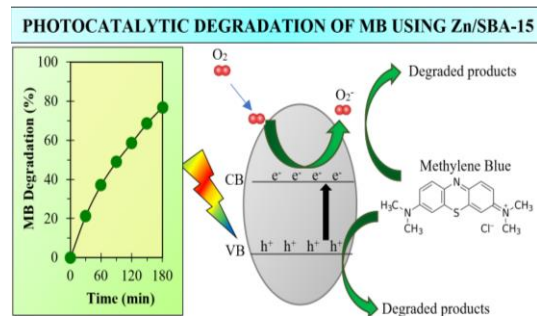
*Corresponding Author: herma@ump.edu.my

Article history :

Received 19 April 2020

Accepted 21 June 2020

GRAPHICAL ABSTRACT



ABSTRACT

This study focused on the potential of Zn/SBA-15 synthesized from POFA for photocatalytic degradation of methylene blue (MB). The synthesized Zn/SBA-15 was characterized using XRD, FESEM, and N₂ adsorption-desorption, and catalytically evaluated for batch photocatalytic of MB at various parameters including effects of time (0–180 min), catalyst dosage (0.5–5 g/L), pH (2–8), and initial MB concentration (10–50 mg/L) under UV light. The characterization analyses disclosed the well formation of SBA-15 and ZnO particles were highly dispersed into/over the well-ordered mesoporous channels. The best conditions were achieved at a time of 180 min, catalyst dosage of 3 g/L, pH 5, and initial MB concentration of 10 mg/L, with MB degradation of 77%. The experimental data demonstrated high linearity with the pseudo-first-order Langmuir-Hinshelwood kinetic model indicating a bimolecular reaction between two species. The results revealed that the synthesized Zn/SBA-15 exhibited excellent catalytic activity towards the photocatalytic degradation of MB dye.

Keywords: photocatalytic; Zn/SBA-15; methylene blue; palm oil fuel ash; kinetic

© 2020 School of Chemical and Engineering, UTM. All rights reserved
| eISSN 0128-2581 |

1. INTRODUCTION

In recent years, industrial wastewater treatment has become more important owing to the high toxicity of the containing pollutants which can seriously damage the environment. An extensive application of dyes was reported at various commercial levels, predominantly in the textile, leather, paper, and cosmetic industries. It is anticipated that roughly more than 107 tons of colors are produced yearly for commercial utilize which comprises of more than 100,000 dyes [1]. Among others, methylene blue (MB) is extensively used in industries and the exposure of MB can result in vomiting, eye infection, diarrhea, and nausea [2].

Several methods have been utilized to eliminate the dyes from wastewater such as biological, chemical, and physical techniques, such as ultrafiltration [3], ion exchange [4], adsorption on various adsorbents [2,5], and photocatalysis [6-9]. Among the above-mentioned methods, photocatalysis has attracted considerable attention for the removal of dyes and other complex pollutants (such as pharmaceuticals) owing to its promising performance. Regarding the choice of photocatalyst, Zinc Oxide (ZnO) is

reported to have comparable potential with commercial TiO₂ owing to its good stability and low cost [6-7]. In addition, ZnO has interesting features than commercial TiO₂ which is higher photocatalytic activities and has a favorable bandgap energy (about 3.2 eV) [8-9].

In the early 1990s, mesoporous silica materials have attracted extraordinary consideration after the discovery of a new family of molecular sieve called M41S. Among others, SBA-type silicas are the utmost regularly explored [9]. The advantages of the use of SBA-15 as photocatalyst support due to its interesting properties including adjustable framework compositions, high thermal stability, and high surface-to-volume ratio [10]. Over the past years, the application of Zn/SBA-15 as photocatalyst has attracted considerable attention on account of its high degradation ability [9,11]. However, due to the high cost of the commercial silica precursor, the application of silica-rich wastes as an alternate silica source seems to be a promising approach to synthesize Zn/SBA-15.

In Malaysia, the palm oil industry produces an enormous amount of oil palm solid wastes including palm oil fuel ash (POFA). Previously, our research group [12] has

successfully synthesized SBA-15 from POFA for catalytic gas reaction. The synthesized SBA-15 having interesting physical and chemical properties, similar to conventional SBA-15. These interesting properties lead to the good distribution of active sites and consequently enhance the catalytic activity of the catalyst. Injunction with this previous study, the present study is to examine the potential of Zn/SBA-15 synthesized from POFA for photocatalytic degradation of methylene blue (MB).

2. EXPERIMENTAL

2.1. Materials

Palm oil fuel ash (POFA) was collected from the palm oil mill in Pahang. Tetraethoxysilane (TEOS) (purity 99%), triblock copolymer EO₂₀PO₇₀EO₂₀ (triblock P123, MW = 5800, Aldrich) and methylene blue (purity 98%) from Sigma Aldrich. Hydrochloric acid (HCl, 37%, Merck), sodium hydroxide powder (purity 97%), and Zn (NO₃)₂·6H₂O from Merck.

2.2. Synthesis of SBA-15

SBA-15 was produced from POFA consistent with the method described in a previous study [12]. In brief, POFA was calcined (600 °C, 6 h) to remove unburnt biomass debris. The calcined POFA was mixed with NaOH solution (2.5 N) and refluxed (80 °C, 3 h) to yield sodium silicate from POFA (Na₂SiO₃-POFA). The Na₂SiO₃-POFA was added dropwise into the mixture of triblock P123 and HCl, and the white precipitate was obtained. The triblock P123 was used as the templating agent, while the HCl was used to keep the medium acidic. The precipitate was rinsed using deionized water, filtered and oven-dried (110 °C, 12 h). The dried solid was calcined (550 °C, 3 h) to produce SBA-15.

2.3. Preparation of Zn/SBA-15

Zn/SBA-15 was prepared employing an incipient wetness impregnation method. In short, SBA-15 was added to a solution of 4 wt% Zn(NO₃)₂·6H₂O (Merck, 99%). The mixture was stirred at 80 °C until all water evaporated. The obtained slurry was oven-dried (110 °C, 12 h) and calcined (500 °C, 4 h).

2.4. Characterization of Zn/SBA-15

The X-ray diffraction (XRD) analysis was performed using RIGAKU XRD (Miniflex II, 15 mA, 30 kV) within the range of 2θ = 0.5°–80°. Meanwhile, Field Emission Scanning Electron Microscopy (FESEM) was carried out by using Zeiss Evo 50. The N₂ adsorption-desorption analysis was examined using AS1 MP-LP analyzer of AUTOSORB-1 model.

2.5. Photocatalytic experiment

The photocatalytic activity of Zn/SBA-15 was evaluated on the degradation of methylene blue (MB) under UV light. The experiments were performed by adding a specific quantity of Zn/SBA-15 into MB solution (200 mL) in a batch reactor fixed with a cooling system and UV lamp (4 × 9 W; 350 nm). The suspension was stirred (700 rpm, 30 min) in a dark condition to achieve adsorption-desorption equilibrium. Then, the suspension was irradiated for 180 min. The suspension was withdrawn at a specific time interval and centrifuged (12,000 rpm, 10 min). The solution was analyzed using a UV-VIS spectrometer at a wavelength of 664 nm. In this study, experiments were carried out various parameters including effects of time (0–180 min), photocatalyst dosage (0.5–5 g/L), pH (2–8), and initial MB concentration (10–50 mg/L). The MB degradation efficiency will be calculated using Eq. (1):

$$MB \text{ Degradation } (\%) = \frac{C_o - C_t}{C_o} \times 100 \quad (1)$$

where C_o is the initial MB concentration at t = 0 (mg/L) and C_t is the MB concentration at a given time (mg/L).

3. RESULTS AND DISCUSSION

3.1. Characterization of Zn/SBA-15

Figure 1(A) shows the low-angle XRD pattern of Zn/SBA-15. As shown, three peaks were observed at about 2θ of 0.9°, 1.7°, and 1.9°, recognized to the (100), (110), and (200) reflections, individually. This indicates the p6mm symmetry of 2D of hexagonal pore arrangement and mesostructured of SBA-15 [9].

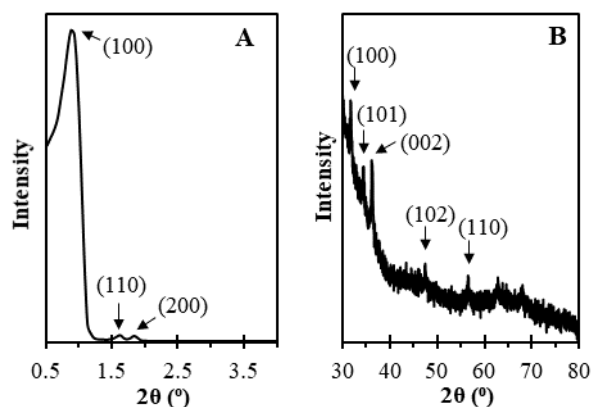


Figure 1: XRD spectra of (A) low-angle and (B) wide-angle of Zn/SBA-15.

The wide-angle XRD pattern of Zn/SBA-15 is shown in Figure 1(B). Five main diffraction peaks were observed at 2θ = 31.76°, 34.41°, 36.24°, 47.53° and 56.58°, which strongly matched with the diffraction planes (100), (002), (101), (102) and (110), correspondingly, as described in the standard spectrum of ZnO (JCPDS No. 01-089-0510). The presence of these sharp diffraction peaks signifying the high

crystallinity of the prepared Zn/SBA-15 catalyst which can increase the photocatalysis activity of Zn/SBA-15 by hindering e^-/h^+ pair recombination and creating additional reactive species for effective reaction with MB molecules. Similar findings reported in the literature [6].

Figure 2 shows the FESEM image of Zn/SBA-15 under 50,000x of magnification. As shown in the figure, Zn/SBA-15 consists of well-defined sphere structures aggregated together with relatively uniform sizes of ~150 nm. Besides, according to the N_2 adsorption-desorption analysis, Zn/SBA-15 has a high BET surface area ($179 \text{ m}^2/\text{g}$) and pore volume ($0.33 \text{ cm}^3/\text{g}$), indicating a good distribution of the Zn particles on the surface of SBA-15. The well distribution of Zn particles will play an important role in the photocatalytic reaction.

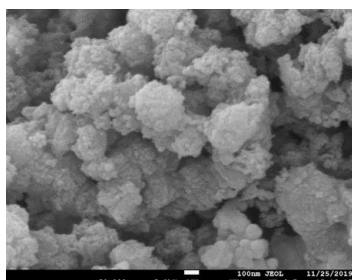


Figure 2: FESEM image of Zn/SBA-15 at magnification of 50,000x

3.2. Photocatalytic activity

Figure 3 displays the degradation of MB with the effect of time. With an increase in time, the degradation of MB was found to increase from 0 to 54% within 180 minutes of the photocatalytic degradation process. Such findings uncover the relatively high activity of the synthesized Zn/SBA-15 catalyst and the catalyst has appropriate active sites for carrying out the reaction. Besides, it is also discovered the high potential of Zn/SBA-15 synthesized from POFA for efficient photocatalytic degradation of MB.

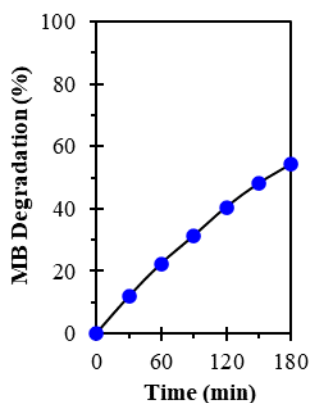


Figure 3: Effect of time on methylene blue using Zn/SBA-15 ($C_o = 20 \text{ mg/L}$; $m = 3 \text{ g/L}$; $\text{pH} = 5$; $T = 30^\circ\text{C}$).

Figure 4 illustrates the effect of the Zn/SBA-15 dosage on the MB degradation. An increase in Zn/SBA-15

dosage up to 3 g/L improved the percentage of MB degradation from 0 to 54%. Beyond this value, the reaction seems to be stable. The increment in degradation efficiency with increasing in Zn/SBA-15 dosage may be attributed to a higher number of available active sites with an increase of Zn/SBA-15 dosage. The relationship between catalyst dosage and the number of active sites for the reaction was also reported in literature [6,9].

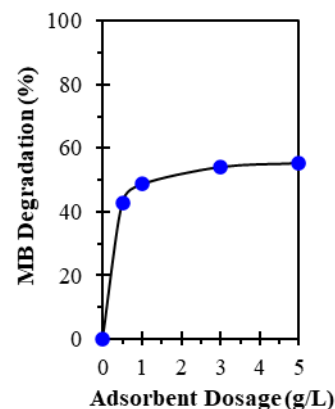


Figure 4: Effect of catalyst dosage of Zn/SBA-15 ($C_o = 20 \text{ mg/L}$; $t = 180 \text{ min}$; $\text{pH} = 5$; $T = 30^\circ\text{C}$).

Figure 5 displays the influence of the pH on the photocatalytic degradation of MB using Zn/SBA-15. pH has a great influence on the photocatalytic degradation process, since it affects not only the charge of catalyst surface but also the dye molecules dissociation. At pH 2, the environment was saturated with the surplus of H^+ ions, thus hindering the adsorption and photodegradation of MB molecules.

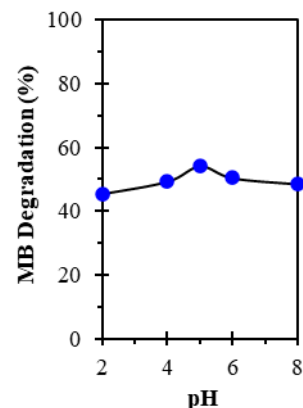


Figure 5: Effect of pH on MB degradation using Zn/SBA-15 ($C_o = 20 \text{ mg/L}$; $t = 180 \text{ min}$; $m = 3 \text{ g/L}$; $T = 30^\circ\text{C}$).

However, lowering the acidic condition from pH 2 to pH 5 may decrease the number of positive charges on the catalyst surface, thus increasing the attraction of MB to the catalyst surface. This phenomenon facilitates the degradation of MB. In contrast, a further increment in pH reduces the photocatalytic activity due to the saturation and high contamination of the MB molecules on the catalyst surface. This phenomenon hindering the light penetration, which is the foremost vital factor for producing an electron-

hole pair. The optimal pH for this process was attained at pH 5. A similar phenomenon on the influence of pH towards degradation percentage of MB was reported by Sapawe et al. [6] for MB decolorization using EGZnO/HY catalyst.

Figure 6 illustrates the impact of the MB initial concentration on the degradation of MB using Zn/SBA-15. As shown, an increase in MB concentration from 10 mg/L to 50 mg/L decreased the percentage degradation of MB from 77% to 26%. This finding due to an important relationship between photocatalytic degradation efficiency and initial MB concentration. The increase in the initial dye concentration subsequently decreases the photons entering solutions due to the decrease of the path length, which results in a lower adsorption for the photon on the catalyst particles, and consequently reducing the degradation efficiency [13]. Besides, at high MB concentrations, there were small changes in degradation efficiency due to the existence of a high quantity of adsorbed MB results in a deficit of direct contact with the holes or hydroxyl free radicals [9].

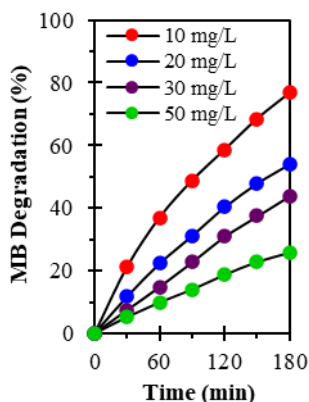


Figure 6: Effect of initial concentration of methylene blue ($t = 180$ min; $pH = 5$; $m = 3$ g/L; $T = 30^\circ\text{C}$).

Table 1 shows the photocatalytic degradation of MB using different catalysts reported in the literature. The synthesized Zn/SBA-15 has comparable degradation efficiency with reported catalysts, indicating the high potential of Zn/SBA-15 synthesized from POFA for MB degradation.

Table 1: Summary of studies using different catalysts on photocatalytic degradation of MB

Catalyst	Degradation (%)	Conditions	Ref.
EGZnO/HY	68	$C_o = 10$ mg/L; $m = 0.375$ g/L; $t = 240$ min; $pH = 3$; $T = 30^\circ\text{C}$, lamp = 420 nm	[6]
MCM-41/ZnO	59	$C_o = 10$ mg/L; $m = 1.0$ g/L; $t = 150$ min; lamp = 400 watt	[7]

ZnO/SBA-15	69	$C_o = 30$ mg/L; $m = 0.13$ g/L; $t = 120$ min; $pH = 7$; $T = 20^\circ\text{C}$; lamp = 254 nm	[9]
ZnO nanoparticles	48	$C_o = 5$ mg/L; $m = 0.15$ g/L; $t = 150$ min; $T = 30^\circ\text{C}$; lamp = 254 nm	[14]
Zn/SBA-15	77	$C_o = 10$ mg/L; $m = 3$ g/L; $t = 180$ min; $pH = 5$; $T = 30^\circ\text{C}$; lamp = 350 nm	This study

3.3. Photocatalytic Kinetics

The kinetic study of photocatalytic degradation of MB using Zn/SBA-15 was modeled by the Langmuir-Hinshelwood model [15]. This model assumes a direct correlation between the occupation rate of sorption sites with the number of unoccupied sites. Generally, the pseudo-first-order equation is expressed in equation (2).

$$\ln\left(\frac{C_o}{C_t}\right) = kt \quad (2)$$

where C_o (mg/L) is the initial MB concentration, C_t (mg/L) is the concentration of the MB at time t , k is the reaction rate constant (min^{-1}), and t is the irradiation time (min).

The k value was determined from the intercept and slope of regression equations and tabulated in Table 2. From the results obtained, the correlation coefficient (R^2) is 0.9936-0.9984. Therefore, the photocatalytic degradation of MB by Zn/SBA-15 well fitted the Langmuir-Hinshelwood pseudo-first-order kinetic model.

Table 2: Kinetic Parameters for photocatalytic degradation of MB using Zn/SBA-15

Concentration (mg/L)	Pseudo-first-order	
	k (min^{-1})	R^2
10	0.0078	0.9955
20	0.0043	0.9994
30	0.0031	0.9936
50	0.0017	0.9984

4. CONCLUSION

Zn/SBA-15 catalyst was successfully prepared using POFA and used for MB degradation using UV light. The characterization results showed the well formation of Zn/SBA-15. The best conditions were achieved at a time of 180 min, photocatalyst dosage of 3 g/L, pH 5, initial MB concentration of 10 mg/L, with MB degradation of 77%. The photocatalytic kinetics well fitted with the Langmuir-Hinshelwood pseudo-first-order reaction model with an R^2 value of 0.9936-0.9994 indicating a bimolecular reaction

between two species available on the catalyst's surface. The results revealed that the Zn/SBA-15 synthesized from POFA exhibited excellent catalytic activity towards the degradation of MB under UV light. As a continuity of this study, the reusability and regeneration of Zn/SBA-15 can be explored. In addition, the photocatalytic activities can be further studied using industrial wastewater containing MB.

ACKNOWLEDGMENTS

Thank you for the monetary support from Universiti Malaysia Pahang through FTA1000.

REFERENCES

- [1] C.H. Huang, K.P. Chang, H.D. Ou, Y.C. Chiang, E.E. Chang, C.F. Wang, *J. Hazard. Mater.* 186(2–3) (2011) 1174.
- [2] R. Hasan, N.A.F. Ahliyasah, C.C. Chong, R. Jusoh, H.D. Setiabudi, *Bull. Chem. React. Eng. Catal.* 14(1) (2019) 158.
- [3] J. Dasgupta, A. Singh, S. Kumar, J. Sikder, S. Chakraborty, S. Curcio, H.A. Arafat, (2016). *J. Env. Chem. Eng.* 4(2) (2016) 2008
- [4] J. Joseph, R.C. Radhakrishnan, J.K. Johnson, S.P. Joy, J. Thomas, *Mater. Chem. Phys.* 242 (2020) 122488.
- [5] L. Sellaoui, D. Franco, H. Ghalla, J. Georgin, M.S. Netto, G.L. Dotto, A. Bajahzar, *Chem Eng. J.* (2020) 125011.
- [6] N. Sapawe, A.A. Jalil, S. Triwahyono, R.N.R.A. Sah, N.W.C. Jusoh, N.H.H. Hairom, J. Efendi, *Appl. Catal. A: Gen.* 456 (2013) 144.
- [7] S.A. El-Hakam, H.Z. El-Shenawy, A.G. Abd-El-Hamid, Z.A. El-Samia, *Int. J. Modern Chem.* 10(2) (2018) 172-184.
- [8] P. Muthirulan, M. Meenakshisundaram, N. Kannan, *J. Adv. Res.* 4(6) (2013) 479.
- [9] L.A. Calzada, R. Castellanos, L.A. García, T.K. Berestneva, *Micro. Meso. Mater.* 285 (2019) 247.
- [10] W. Stevens, K. Lebeau, M. Mertens, G. van Tendeloo, P. Cool, E. Vansant, *J. Phy. Chem. B*, 110 (18) (2006) 9183.
- [11] V. Vo, T.P.T. Thi, H.Y. Kim, S.J. Kim, *J. Phys. Chem. Solids.* 75(3) (2014) 403.
- [12] C.C. Chong, N. Abdullah, S.N. Bukhari, N. Ainirazali, L.P. Teh, H.D. Setiabudi, *Int. J. Hydrogen Energ.* 44(37) (2019) 20815.
- [13] N.F. Jaafar, A.A. Jalil, S. Triwahyono, M.N.M. Muhid, N. Sapawe, M.A.H. Satar, H. Asaari, *Chem. Eng. J.* 191 (2012) 112.
- [14] M.S. Azmina, R. Md Nor, H.A. Rafeaie, N.S.A. Razak, S.F.A. Sani, Z. Osman, *Appl. Nanosci.* 7(8) (2017) 885.
- [15] C.S. Turchi, D.F. Ollis, *J. Catal.*, 122 (1990) 178.